THE JOURNAL OF PHYSICAL CHEMISTRY A

Article

pubs.acs.org/JPCA

Substituent Effects in the Noncovalent Bonding of SO_2 to Molecules Containing a Carbonyl Group. The Dominating Role of the Chalcogen Bond

Luis Miguel Azofra[†,‡] and Steve Scheiner*[,‡]

[†]Instituto de Química Médica, CSIC, Juan de la Cierva, 3, E-28006, Madrid, Spain

[‡]Department of Chemistry and Biochemistry, Utah State University, Logan, Utah 84322-0300, United States

Supporting Information

ABSTRACT: The SO_2 molecule is paired with a number of carbonyl-containing molecules, and the properties of the resulting complexes are calculated by high-level *ab initio* theory. The global minimum of each pair is held together primarily by a S···O chalcogen bond wherein the lone pairs of the carbonyl O transfer charge to the π^* antibonding SO orbital, supplemented by smaller contributions from weak CH···O H-bonds. The binding energies vary between 4.2 and 8.6 kcal/mol, competitive with even some of the stronger noncovalent forces such as H-bonds and halogen bonds. The geometrical arrangement places the carbonyl O atom above the plane of the SO_2 molecule, consistent with the disposition of the molecular electrostatic potentials of the two monomers. This S···O bond differs from the more commonly observed chalcogen bond in both geometry and origin. Substituents exert their influence via inductive effects that change the availability of the carbonyl O lone pairs as well as the intensity of the negative electrostatic potential surrounding this atom.

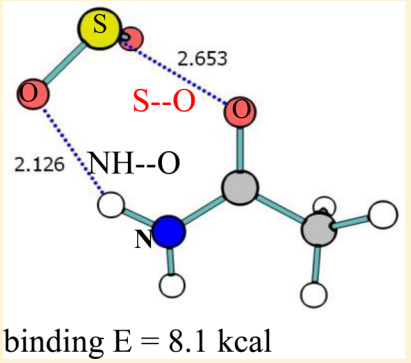

INTRODUCTION

Within the regime of noncovalent bonds, there is growing interest in attractive forces between electronegative atoms. Once thought to be counterintuitive on the basis of Coulombic repulsion between two negatively charged atoms, this idea was countered by more detailed examination of the charge distribution. Taking the halogen atom X as an example, a band of negative charge around its equator encircles a positive pole region, directly opposite the C−X bond. The latter positive region can attract a negative region of another molecule, forming what is commonly termed a halogen bond.[1−10] This phenomenon is not limited to halogens, but has been observed in the cases of pnicogen[11−20] and chalcogen[21−31] atoms, and perhaps even the tetrel atoms of the C family as well.[32−35]

Along with the electrostatic attraction, these bonds typically contain a strong induction element, attributed primarily to charge transfer from a lone pair of the partner Lewis base to the σ^*(C−X) antibonding orbital of the electron acceptor. Both the electrostatic and charge transfer components favor the approach of the electron donor along the C−X direction. However, there are other molecules which present a somewhat more complicated situation. SO_2 is such a case, where the central S atom is involved in a pair of double bonds. When paired with CO_2, two different geometries were observed[36] as minima, not very different in energy. In the global minimum, SO_2 serves as electron donor, with its O lone pairs contributing charge to the π^*(CO) orbitals, with little involvement of the central S. The other minimum also manifested this same shift, but one that was supplemented by a smaller transfer in the opposite direction, from the CO_2 O lone pairs to a π^*(SO) antibond. It is the latter sort of transfer that becomes dominant when SO_2 is paired with a stronger electron donor H_2CO.[37] This H_2CO $O_{lp} \rightarrow \pi^*$(SO) shift is manifested as a S···O chalcogen bond, but one that differs from the usual sort. Rather than approaching SO_2 along a S═O direction, the carbonyl prefers a position above the SO_2 plane, and instead of the usual transfer into a σ^* orbital, it is an SO π^* orbital which is the recipient of this charge. This region in SO_2 has been described as a π-hole[38] and its ability to enhance the presence of weak interactions has also been described between CO_2 (classical π-hole system) and carbonyl compounds.[39,40]

The question then arises as to whether this unusual sort of S···O bond is typical of the interaction of SO_2 with any carbonyl-containing molecule, or is confined only to H_2CO. What might be the effects of replacing the H atoms of H_2CO by various different substituents? Will the S···O chalcogen bond remain as the dominant interaction, or will it be replaced by other, perhaps stronger, forces such as H-bonds (HBs), for example? How might the strength of this chalcogen bond be affected by the properties of various substituents? What is the limit of the strength of this unusual sort of chalcogen bond, first in comparison with the more common type of chalcogen bond, but also with respect to HBs, halogen bonds, and so forth, that

Received: February 24, 2014
Revised: April 28, 2014
Published: May 2, 2014

dx.doi.org/10.1021/jp501932g | J. Phys. Chem. A 2014, 118, 3835−3845

are commonly mentioned as important ingredients in crystal engineering?

It is the goal of this work to answer some of these questions. SO_2 is paired with a group of carbonyl-containing molecules, ranging from simple methyl substitution, as in $HCOCH_3$, to amides and esters, to more complicated systems like $CH_3COOCOCH_3$ and $CH_3CONHCOCH_3$. Calculations locate all minima on the potential energy surface (PES) of each pair, and each is carefully analyzed to identify the nature of its intermolecular binding. The effects of substituents are compared and related to their fundamental inductive properties. The S···O bond is found to dominate most of the more strongly bound complexes, even the secondary minima. The binding energies vary between 4 and 9 kcal/mol, making this type of S···O chalcogen bond competitive with even some of the stronger HBs, such as NH···O interaction.

COMPUTATIONAL METHODS

SO_2 was paired with a series of molecules containing a carbonyl group. The geometries were optimized and properties extracted from second-order Møller−Plesset[41] perturbation theory (MP2) calculations using the aug-cc-pVDZ[42−44] basis set. Searches of the PES were carried out first by using the molecular electrostatic potential (MEP) of each monomer as a guide, followed by a random selection of other starting points.[45] After optimization of each of the 50 starting points using MP2/cc-pVDZ, any geometries not already identified by the first set were reoptimized using the full MP2/aug-cc-pVDZ formalism. All structures were verified as true minima by virtue of all positive vibrational frequencies, which were then used to compute zero-point vibrational energies (ZPE). All calculations were carried out with the GAUSSIAN-09 program.[46]

Interaction energies, E_{int}, were computed as the difference in energy between the complex on one hand and the sum of the energies of the two monomers on the other, using the monomer geometries from the optimized complex. Interaction energies were corrected for basis set superposition error (BSSE) by the counterpoise procedure (CP). Single-point MP2/aug-cc-pVTZ calculations were performed, using MP2/aug-cc-pVDZ geometries so as to obtain more accurate interaction energies. Slightly different in formalism, binding energies, E_b, were computed as the difference in energy between the complex on one hand, and the sum of the energies of the optimized monomers on the other, also taking into account the ZPE.

Atoms in molecules (AIM) theory[47,48] at MP2-level, and natural bond orbital (NBO) theory[49] with the ωB97XD functional,[50] were applied to help analyze the interactions, using the AIMAll[51] and NBO6.0 programs.[52]

RESULTS AND DISCUSSION

Monomers. The carbonyl chemical functionality (C═O) was examined within $HCOCH_3$, **1**; CH_3COCH_3, **2**; $HOCOCH_3$, **3**; CH_3OCOCH_3, **4**; H_2NCOCH_3, **5**; $(CH_3)_2NCOCH_3$, **6**; $CH_2CHCOCH_3$, **7**; $FCOCH_3$, **8**; $ClCOCH_3$, **9**; $BrCOCH_3$, **10**; $CH_3COOCOCH_3$, **11**; and $CH_3CONHCOCH_3$, **12**. MEP of each of these monomers is illustrated in Figure S1 of the Supporting Information (SI), where red and blue regions correspond to the extreme negative and positive potentials, respectively.

Structures and Binding. In our previous work,[37] we found that the simple $H_2CO:SO_2$ heterodimer has only one minimum with an interaction energy of −5.42 kcal/mol at the CCSD(T)/aug-cc-pVTZ//MP2/aug-cc-pVDZ computational level. This dimer serves as a reference point for the other complexes discussed below and so is pictured in Figure 1, in which broken

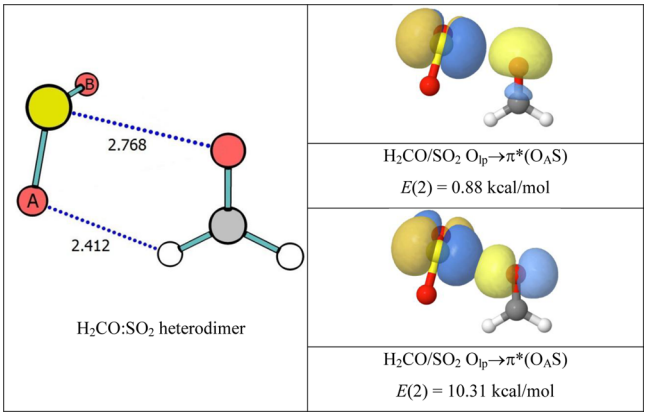

Figure 1. $H_2CO:SO_2$ heterodimer at MP2/aug-cc-pVDZ computational level and its main $O_{lp} \rightarrow \pi^*(O_AS)$ NBO interactions. Blue dot lines link atoms which present interatomic AIM BCPs, with interatomic distances in Å.

blue lines on the left indicate AIM bond critical points (BCP) linking pairs of atoms. NBO analysis on the right indicates the principal interaction involves an $O_{lp} \rightarrow \pi^*(SO)$ charge transfer from H_2CO to SO_2, supplemented by a weaker CH···O HB. The values of $E(2)$ for these two interactions are 11.19 and 2.08 kcal/mol, respectively. The former is illustrated in the right panels of Figure 1, separating the interaction into the pieces from each of the two O lone pairs.

Each of the carbonyl-containing molecules **1**−**12** formed multiple minima with SO_2, leading to 51 different structures in all. The numbering system refers to complexes with aldehyde $HCOCH_3$ as **1a** and **1b**, those with ketone CH_3COCH_3 as **2a** and **2b**, and so forth. The interaction and binding energies for all minima located on each surface are gathered in Table 1, using both the aug-cc-pVDZ and aug-cc-pVTZ basis sets at the MP2 level.

Replacement of one H atom of H_2CO by a methyl group leads to complex **1a** which is quite similar to the $H_2CO:SO_2$ complex in Figure 1. The only difference is a quantitative one, with somewhat shorter interatomic distances in **1a**, suggesting that the methyl group strengthens the interaction. And indeed, the interaction energy of **1a** amounts to 4.97 kcal/mol after CP correction at the MP2/aug-cc-pVDZ level, as compared to 4.41 kcal/mol for the simpler $H_2CO:SO_2$. As an electron-releasing agent, the methyl group could be adding density to the O lone pairs which augments the donation to the $\pi^*(OS)$ orbital of SO_2. The values of $E(2)$ for **1a**, and all other global minima, are reported in Table 2. **1b** is similar to **1a** in that it also contains an $O_{lp} \rightarrow \pi^*(OS)$ chalcogen bond, but it differs in that the CH···O HB involves a methyl CH. Since the latter is less activated than the aldehydic CH, this HB is longer by 0.27 Å, and the entire complex bound by about 0.9 kcal/mol less. This difference is confirmed by NBO analysis in that the $O_{lp} \rightarrow \sigma^*(CH)$ $E(2)$ drops from 2.60 kcal/mol in **1a** down to 1.06 kcal/mol in **1b**. The values of $E(2)$ are reported for all minima in Table S1 of the SI. The O···S distance is also longer in **1b**, reflected by a reduction in $O_{lp} \rightarrow \pi^*(OS)$.

dx.doi.org/10.1021/jp501932g | J. Phys. Chem. A 2014, 118, 3835−3845

Table 1. Binding (E_b) and Interaction (E_{int}) Energies in kcal/mol for the Heterodimer Complexes at the MP2/aug-cc-pVDZ Level, And Interaction Energies at MP2/aug-cc-pVTZ (Single Point) Computational Level

		aug-cc-pVDZ					aug-cc-pVTZ	
compound	symmetry	E_b	E_b[a]	E_b[b]	E_{int}	E_{int}[b]	E_{int}	E_{int}[b]
1a	C_1	−6.90	−5.72	−4.97	−7.00	−5.07	−6.74	−5.91
1b	C_1	−6.08	−5.19	−4.27	−6.21	−4.40	−5.88	−5.03
2a	C_1	−6.95	−5.94	−4.79	−7.18	−5.02	−6.74	−5.77
2b	C_{2v}	−3.44	−2.90	−1.87	−3.46	−1.89	−3.05	−2.19
3a	C_1	−7.44	−6.45	−5.36	−7.71	−5.63	−7.51	−6.46
3b	C_1	−6.43	−5.56	−4.36	−6.76	−4.69	−6.32	−5.39
3c	C_s	−4.78	−4.15	−3.03	−4.86	−3.11	−4.48	−3.61
3d	C_1	−4.51	−3.94	−2.85	−4.58	−2.92	−4.16	−3.38
4a	C_s	−7.11	−6.23	−4.92	−7.24	−5.05	−6.68	−5.68
4b	C_s	−7.02	−6.07	−4.79	−7.36	−5.13	−6.90	−5.91
4c	C_1	−6.88	−6.03	−4.46	−7.12	−4.70	−6.53	−5.43
4d	C_1	−5.95	−5.26	−3.44	−6.07	−3.56	−5.37	−4.27
4e	C_s	−5.43	−4.79	−3.26	−5.51	−3.34	−5.01	−3.99
4f	C_1	−5.40	−4.77	−2.93	−5.49	−3.02	−4.74	−3.70
5a	C_1	−9.04	−7.64	−6.76	−9.37	−7.09	−9.21	−8.14
5b	C_s	−8.32	−7.11	−6.00	−8.55	−6.23	−8.21	−7.19
5c	C_1	−4.57	−3.73	−2.92	−4.63	−2.98	−4.22	−3.26
5d	C_1	−4.54	−3.65	−2.91	−4.57	−2.94	−4.13	−3.18
5e	C_1	−4.27	−3.42	−2.31	−4.34	−2.38	−3.63	−2.73
5f	C_s	−4.22	−3.36	−2.80	−4.29	−2.87	−3.85	−3.06
6a	C_1	−10.90	−9.65	−6.36	−11.37	−6.83	−10.50	−8.55
6b	C_1	−10.44	−9.26	−6.74	−10.95	−7.25	−10.04	−8.46
6c	C_1	−10.17	−9.13	−6.48	−10.65	−6.96	−9.65	−8.09
6d	C_1	−9.17	−8.06	−4.67	−9.69	−5.19	−8.69	−6.77
6e	C_1	−3.76	−3.30	−1.84	−3.80	−1.88	−3.17	−2.18
7a	C_1	−7.32	−6.47	−4.63	−7.71	−5.02	−7.09	−5.90
7b	C_1	−6.84	−6.01	−4.66	−7.01	−4.83	−6.58	−5.57
7c	C_1	−6.34	−5.73	−3.70	−6.49	−3.85	−5.66	−4.54
7d	C_1	−4.97	−4.43	−2.49	−5.02	−2.54	−4.30	−3.16
7e	C_s	−2.24	−1.84	−0.54	−2.25	−0.55	−1.44	−0.76
8a	C_1	−5.51	−4.78	−3.69	−5.64	−3.82	−5.21	−4.34
8b	C_1	−5.10	−4.57	−2.99	−5.17	−3.06	−4.40	−3.49
8c	C_1	−4.71	−4.16	−2.80	−4.82	−2.91	−4.27	−3.32
8d	C_s	−4.64	−4.08	−3.00	−4.75	−3.11	−4.38	−3.55
9a	C_1	−5.47	−4.94	−3.25	−5.52	−3.30	−4.77	−3.82
9b	C_1	−5.37	−4.71	−3.48	−5.48	−3.59	−5.05	−4.12
9c	C_1	−5.32	−4.72	−3.16	−5.48	−3.32	−4.94	−3.90
9d	C_s	−4.85	−4.28	−3.22	−4.97	−3.34	−4.66	−3.79
10a	C_1	−5.87	−5.25	−3.32	−6.05	−3.50	−5.74	−4.24
10b	C_1	−5.84	−5.31	−3.32	−5.92	−3.40	−5.44	−4.05
10c	C_1	−5.35	−4.72	−3.37	−5.43	−3.45	−5.07	−3.98
10d	C_s	−5.29	−4.70	−3.24	−5.42	−3.37	−5.29	−4.07
10e	C_s	−2.53	−2.29	−1.34	−2.54	−1.35	−2.34	−1.67
11a	C_1	−8.63	−7.75	−5.49	−8.92	−5.78	−7.89	−6.56
11b	C_1	−7.98	−7.18	−5.03	−8.33	−5.38	−7.42	−6.10
11c	C_1	−7.79	−7.02	−4.76	−8.05	−5.02	−7.17	−5.79
11d	C_1	−6.23	−5.53	−4.20	−6.38	−4.35	−5.87	−4.93
11e	C_1	−5.57	−5.01	−2.76	−5.74	−2.93	−4.84	−3.60
12a	C_1	−10.13	−9.11	−6.70	−10.58	−7.15	−9.49	−8.05
12b	C_1	−7.71	−6.73	−5.35	−8.07	−5.71	−7.56	−6.52
12c	C_1	−6.22	−5.42	−3.93	−6.29	−4.00	−5.62	−4.32

[a]Inclusion of the zero point energy (ZPE). [b]With counterpoise correction of the basis set superposition error (BSSE).

Turning next to ketone **2** wherein both H atoms of H_2CO are replaced by methyls, we see that its global minimum **2a** continues the S···O chalcogen bond, but does not have an aldehydic CH proton donor, so must resort instead to a methyl CH···O interaction. This HB is both weaker, with a reduced $E(2)$, and 0.3 Å longer. The $O_{lp} \rightarrow \pi^*(OS)$ charge transfer is also weakened in **2a** relative to **1a**, and the S···O distance is consequently lengthened. AIM analysis suggests a C···O bond, which fits into the category of what has been termed a "tetrel bond" of late, although NBO does not support this

dx.doi.org/10.1021/jp501932g | J. Phys. Chem. A 2014, 118, 3835−3845

Table 2. Second-Order Perturbation NBO Energy, $E(2)$ in kcal/mol, for the Structures in Figure 2, at the ωB97XD/aug-cc-pVDZ Computational Level

compound	donor/acceptor	type	$E(2)$
1a	sol./SO_2	$O_{lp}\rightarrow\pi^*(SO)$	11.90
	SO_2/sol.	$O_{lp}\rightarrow\sigma^*(CH)$	2.60
2a	sol./SO_2	$O_{lp}\rightarrow\pi^*(SO)$	8.00
	SO_2/sol.	$\pi(SO)\rightarrow\sigma^*(CH)$	0.59
3a	sol./SO_2	$O_{lp}\rightarrow\pi^*(SO)$	6.89
	SO_2/sol.	$O_{lp}\rightarrow\sigma^*(CH)$	10.70
4b	sol./SO_2	$O_{lp}\rightarrow\pi^*(SO)$	10.72
5a	sol./SO_2	$O_{lp}\rightarrow\pi^*(SO)$	16.09
	SO_2/sol.	$O_{lp}\rightarrow\sigma^*(NH)$	7.35
6a	sol./SO_2	$N_{lp}\rightarrow\sigma^*(SO)$	1.03
	sol./SO_2	$N_{lp}\rightarrow\pi^*(SO)$	22.20
	SO_2/sol.	$O_{lp}\rightarrow\sigma^*(CH)$	1.55
7a	sol./SO_2	$O_{lp}\rightarrow\pi^*(SO)$	3.15
	sol./SO_2	$\pi(CO)\rightarrow\pi^*(SO)$	3.03
	SO_2/sol.	$O_{lp}\rightarrow\pi^*(CO)$	0.80
8a	sol./SO_2	$O_{lp}\rightarrow\pi^*(SO)$	4.09
	SO_2/sol.	$O_{lp}\rightarrow\sigma^*(CH)$	0.76
9b	sol./SO_2	$O_{lp}\rightarrow\pi^*(SO)$	2.39
	SO_2/sol.	$O_{lp}\rightarrow\sigma^*(CH)$	0.66
10a	sol./SO_2	$Br_{lp}\rightarrow\pi^*(SO)$	3.00
	SO_2/sol.	$O_{lp}\rightarrow\sigma^*(CH)$	1.50
	SO_2/sol.	$\pi(SO)\rightarrow\pi^*(CO)$	1.03
11a	sol./SO_2	$O_{lp}\rightarrow\pi^*(SO)$	5.34
	SO_2/sol.	$O_{lp}\rightarrow\pi^*(CO)$	2.29
12a	sol./SO_2	$O_{lp}\rightarrow\pi^*(SO)$	3.94
	sol./SO_2	$\pi(CO)\rightarrow\pi^*(SO)$	1.71
	SO_2/sol.	$O_{lp}\rightarrow\pi^*(CO)$	1.95

phenomenon. Despite these weaker bonds, **2a** is only about 0.1 kcal/mol more weakly bound that **1a**. Structure **2b** is much weaker, which is not surprising since it is held together only by CH···O HBs. The latter are rather long at 2.773 Å, to the point where $E(2)$ is beneath the usual 0.5 kcal/mol threshold.

Replacement of one of the methyl groups of ketone **2** by a hydroxyl adds a strong proton donor in the form of carboxylic acid **3**. **3a** is thus held together largely by a strong OH···O HB, with R(H···O) less than 2 Å, and $E(2)$ of 10.7 kcal/mol. Supplementing this force is a S···O chalcogen bond, again due to $O_{lp} \rightarrow \pi^*$(OS) charge transfer. This duo of strong noncovalent bonds leads to a high binding energy in **3a** of some 6.5 kcal/mol. The other three local minima of carboxylic acid **3** with SO_2 forego the OH···O HB and are consequently more weakly bound. **3b** retains the S···O bond of **3a**, but replaces OH···O by a weaker methyl CH···O HB, as well as a C···O tetrel bond, resulting in a net reduction of binding energy by 1.1 kcal/mol. **3c** and **3d** are held together principally by CH···O HBs, and a weaker S···O bond to the hydroxylic O.

Replacement of the carboxylic proton by a methyl group removes the possibility of proton donation in the ester **4**. The OH···O HB of **3a** is thus replaced by a pair of weaker CH···O HBs in **4b**, dropping the binding energy down by 0.5 kcal/mol. **4a** is very similar to **4b**, making use of HBs from the other methyl group. In fact, these two structures are quite similar energetically, and their relative stability is reversed by using the slightly smaller basis set. In fact, all six minima on the CH_3COOCH_3:SO_2 PES contain CH···O HBs in concert with S···O chalcogen bonds.

The −COOH group is more acidic than the corresponding amide $-CONH_2$, so the NH···O HB of **5a** is a bit longer than the corresponding OH···O HB of **3a**. On the other hand, the replacement of −OH by $-NH_2$ enhances the electron-donating properties of the O atom (see below). As a result, the S···O distance in **5a** is 0.14 Å shorter than in **3a**, and the $O_{lp} \rightarrow \pi^*$(OS) $E(2)$ is more than double. The net result is a stronger binding energy, by 1.6 kcal/mol. It is this combination of NH···O HB and S···O chalcogen bond which is more effective. Removal of either in the secondary minima yields a weaker interaction, even if replaced by multiple CH···O, or even what AIM designates as a N···O bond in **5f**.

Whereas the replacement of carboxylic H by CH_3 reduced the binding to SO_2, the opposite is true for the amide. Changing both NH protons to methyl groups leads to a small enhancement. **6a** is slightly more strongly bound than is **5a**. NBO analysis traces the binding in **6a** to $N_{lp} \rightarrow \pi^*$(OS), whose large value of $E(2)$ of 22.2 kcal/mol is due to the readiness of the N atom to donate electron density from its lone pair. This strong N···S bond is complemented by a pair of weaker CH_3 CH···O HBs. This same combination of forces is observed in structure **6d**, less stable than **6a** by 1.8 kcal/mol. The second most stable dimer, barely 0.1 kcal/mol higher in energy, relies principally on a new sort of interaction, one in which a CO π-bonding orbital is the source of charge transfer to a SO π^* antibonding orbital, with $E(2)$ for π(OC) $\rightarrow \pi^*$(SO) amounting to 7.9 kcal/mol. The AIM interpretation of this transfer is a simple S···O chalcogen bond, so does not distinguish from the $O_{lp} \rightarrow \pi^*$(OS) transfers discussed earlier. This same force is observed in **6c** as well. **6e** is quite different in that it depends solely on CH_3 CH···O HBs, and is consequently much more weakly bound.

Ketone **7** facilitates analysis of the effects of alkyl chain length upon complexation with SO_2. One of the methyl groups of **2** has been replaced with an ethyl. The global minimum **7a** is much like **2a** in that they both contain a S···O chalcogen bond although it is a bit longer in **7a**, and weaker according to NBO. Interestingly, the usual $O_{lp} \rightarrow \pi^*$(OS) transfer characterizing this bond is augmented by transfer from the CO π bond with an $E(2)$ of 3.0 kcal/mol and smaller $O_{lp} \rightarrow \pi^*$(CO) back transfer from SO_2 to the carbonyl. Like **2a**, **7a** also contains an AIM C···O BCP, for which there is no evidence in the NBO analysis. **7b** is 0.3 kcal/mol higher in energy, and substitutes a CH_3 CH···O HB for some of the other charge transfers. The $SO_2 \rightarrow$ carbonyl back transfer recurs in **7c**, this time with the charge moving into the CO σ^* orbital. **7d** is interesting in that a C═C π bond is the source of transfer into a π^*(OS), with a smaller contribution from a π(SO) into the CO π^* antibond. It is this pair of transfers which likely manifest themselves as C···S and C···O AIM bonds, respectively. **7e** is much more weakly bound, relying entirely on CH···O and CH···S HBs.

The next three monomers replace the aldehydic H by a halogen atom, but the F or Cl plays no direct role in either global minimum. The fluorine and chlorine global minima, **8a** and **9b** contain a S···O chalcogen bond, supplemented by a CH···O. The situation is different for **10a** where the Br atom is intimately involved in the global minimum **10a** via a $Br_{lp} \rightarrow \pi^*$(SO) transfer, translated by AIM into a Br···S bond, and **10a** is slightly more strongly bound than **8a** or **9b**. Such a X···S bond appears for X = F and Cl, but only in secondary minima and with much smaller values of $E(2)$. Also present in global minimum **10a** is a CH···O and π(SO) $\rightarrow \pi^*$(CO) transfer, characterized as a C···O bond by AIM. It may be slightly

dx.doi.org/10.1021/jp501932g | J. Phys. Chem. A 2014, 118, 3835−3845

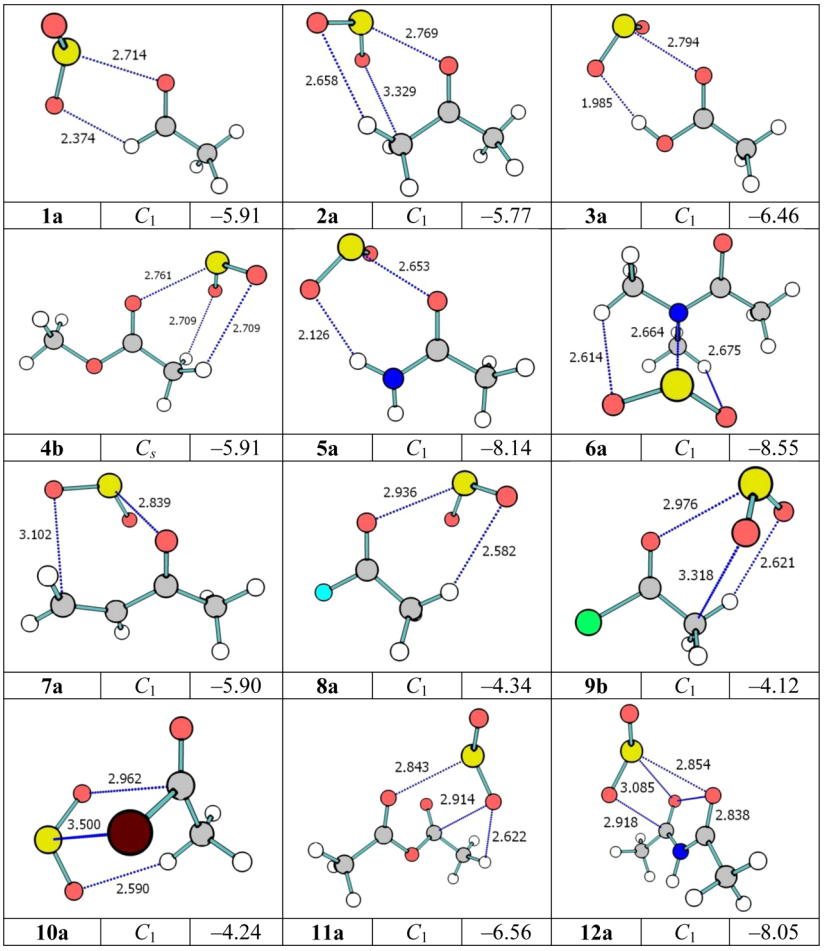

Figure 2. Global minimum for the heterodimers at MP2/aug-cc-pVDZ computational level. Broken blue lines link atoms which present interatomic AIM BCPs, with interatomic distances in Å. Scaling based on E_{int} + BSSE at MP2/aug-cc-pVTZ computational level (single point), in kcal/mol.

surprising to note the absence of any halogen-bonded minima for **9** or **10**. We ascribe this absence in part to the nature of the electrostatic potential. Figure S1 shows that this potential is more positive in the region above the plane, and around the methyl group, than in the vicinity of the Cl or Br atom. This distinction is confirmed by a more quantitative analysis of the MEP, described below. The second factor is the availability of the π^* orbital above the molecular plane which acts to accept electrons from the electronegative O atoms of SO_2.

10e is important because of its superficial geometric resemblance to a halogen bond, with a θ(C−Br···O) angle approaching linearity. However, unlike a halogen bond where charge is transfer to the halogen, **10e** sees transfer in the opposite direction, from a Br lone pair to a σ^*(SO) antibond. This lack of a halogen bond explains the weakness of the binding in **10e** since a halogen bond, particularly one involving Br, would be expected to be many times stronger. And indeed, it is perhaps surprising that there are no halogen bonds in any of these geometries, global or secondary minimum, for any halogen atom, given their proven potential strength. Their absence here is due to the unique electronic structure of SO_2, different than a typical Lewis base which serves as an excellent partner in halogen bonds. Perhaps more importantly, MEP of the $XCOCH_3$ monomers does not indicate the presence of a positive region, or σ-hole,[53] along the extension of the C−X bond (see Figure S1).

The OCOCO linkage containing a pair of carbonyl groups was also examined as a partner to SO_2. The bonding in **11a** is attributed by NBO to both $O_{lp} \rightarrow \pi^*$(SO) and $O_{lp} \rightarrow \pi^*$(CO) transfer in the reverse direction. The latter is observed as a C···O bond by AIM, which also finds a weak CH···O HB. **11b** is only marginally different, mainly in terms of the direction of the second O atom of SO_2 which does not participate directly in any bonds. **11c** contains a pair of AIM O···O bonds, neither of which are confirmed by NBO, which suggests only S···O interaction and a CH···O HB. **11d** and **11e** are still less stable, again incorporating CH···O HBs, in addition to the chalcogen bond.

The replacement of the central O atom of **11** by NH leads to molecule **12**. In addition to the usual $O_{lp} \rightarrow \pi^*$(SO), **12a** also contains both π(CO) → π^*(SO) and $O_{lp} \rightarrow \pi^*$(CO). These orbital interactions appear within the AIM context as a pair of S···O bonds and one C···O interaction. **12b** is less stable, containing only $O_{lp} \rightarrow \pi^*$(SO) although AIM suggests the presence of CH···O bonds as well. **12c**, even higher in energy, is stabilized by a CH···O and NH···O HBs. Perhaps surprisingly, the nominally strong NH···O HB in **12c**, with R(H···O) = 2.105 Å, does not keep this configuration from being the least stable of the three. This observation is another reflection of the low basicity of SO_2.

Surveying these results, we see that the S···O chalcogen bond appears to be a common thread, present in the most stable minimum of each heterodimer, so may be considered a

dx.doi.org/10.1021/jp501932g | J. Phys. Chem. A 2014, 118, 3835−3845

mainstay of these dimers. There is some variability in terms of R(S···O) separation, which varies from a minimum of 2.65 Å for the amide **5**, up to 3.02 Å for the Br substituent **10**. This variability matches well with $E(2)$ $O_{lp} \rightarrow \pi^*(SO)$, which is as large as 16 kcal/mol for **5a**, and drops down near the 0.5 kcal/mol threshold for **10c**. The O lone pairs are not the only possible source for this transfer, which can also involve the π(CO) bond, or a N or halogen lone pair when these atoms are present, and even a π(CC) bond. One sees in certain cases also a reverse transfer from the SO_2 O lone pairs or π(SO) to an antibonding CO orbital of the carbonyl. Regardless of these NBO distinctions, AIM characterizes all such interactions as a S···O noncovalent bond.

Of course, this S···O bond is usually not the only bond present in any of these structures, so cannot be considered the sole source of binding. CH···O HBs are present in many of these dimers, with charge being donated not only from lone pairs but also from π bonding orbitals. There is also a NH···O HB present in some cases, although this bond is surprisingly weak, attributed to the weak basicity of the SO_2 O atoms. C···O bonds, and even C···S, appear in the AIM analysis of some, as well as O···O and N···O, although NBO treatment is not always consistent with this interpretation. Given their potential strength, it is surprising to observe no halogen bonds, even in secondary minima.

Energetics. Various measures of the strengths of the interactions are reported in Table 1. The first five columns of data refer to the MP2/aug-cc-pVDZ level, while the larger aug-cc-pVTZ basis set was used in the final two columns (using the MP2/aug-cc-pVDZ geometries). Binding energies (referred to optimized monomer geometries) are reported first, followed by ZPE corrections and BSSE. These values are followed by the interaction energies, which are similar with the reference being geometries of the monomers within the complex.

There are several points to make about these energies. In the first place, the binding and interaction energies are quite similar to one another, differing between 0.01 and 0.52 kcal/mol, or between 0.4 and 5.4%, indicating little deformation of the monomer geometries upon forming the dimer. The orders of stability of the various complexes are identical whether considering binding or interaction energy, nor is the ordering pattern altered to any appreciable degree by inclusion of ZPE.

The expansion of the basis set from aug-cc-pVDZ to aug-cc-pVTZ increases the CP-corrected interaction energy by an amount between 0.2 and 1.7 kcal/mol, i.e., about 14% on average. In cases where the energies of different configurations are close to one another, there are occasions where the upgrading of the level of theory can cause a reversal. In most cases, however, such a change does not affect the identity of the global minimum. An exception to this rule arises, for instance, in amide **6**: whereas **6b** is more stable than **6a** by 0.4 kcal/mol at the counterpoise-corrected MP2/aug-cc-pVDZ level, the latter is lower in energy by 0.1 kcal/mol when computed with the larger basis set.

The interaction energies fall generally into one of several categories. The N-containing molecules **5**, **6**, and **12** form the strongest interactions, all more than 8 kcal/mol. Molecule **11**, with its pair of carbonyl O atoms, is next most strongly bound at 6.6 kcal/mol, closely followed by carboxylic acid **3**. Aldehyde **1**, ester **4**, and ketones **2** and **7** are bunched rather closely, just less than 6 kcal/mol. The most weakly bound are the halogen-containing molecules **8**, **9**, and **10**, all bound by just a little over 4 kcal/mol.

One's first inclination upon noting the strong complexes arising with the N-containing molecules might lead to the supposition of a strong NH···O HB. However, this bond is rather weak for complexes with SO_2, and in fact is not even present in the global minimum of **12**. It is significant as well that these N-containing molecules form stronger interactions with SO_2 than even the carboxylic group of **3** which is a strong acid. These observations add further weight to the notion that the S···O chalcogen bond is a more dominant factor than even the usually strong NH···O or OH···O HBs. Some of this behavior might be better understood in recalling that the carbonyl molecule serves as electron acceptor in a HB, but is a donor in the chalcogen bond. A NH_2 or $N(CH_3)_2$ substituent as occurs in **5** or **6** is generally considered an electron-releasing agent, so ought to strengthen the chalcogen bond. This expectation is confirmed by the NBO values of $E(2)$ for these bonds, which are the highest of the complexes considered here, consistent with the strong interaction energies. The reverse is true for O-containing substituents such as electron-withdrawing agents carboxyl **3** or ester **4**, where reduced values of $E(2)$ for the chalcogen bonds result in weaker binding. Even more dramatic reductions in chalcogen bond $E(2)$ and consequently total binding energy occurs for the electron-withdrawing halogens **8**, **9**, and **10**.

Electrostatic Potentials. An alternate means of understanding the preferred geometries of the various complexes and their binding strengths is derived from inspection of the electrostatic potentials that surround each monomer. These potentials are illustrated in Figure S1 for all monomers, with several selected potentials displayed in Figure 3. The potential

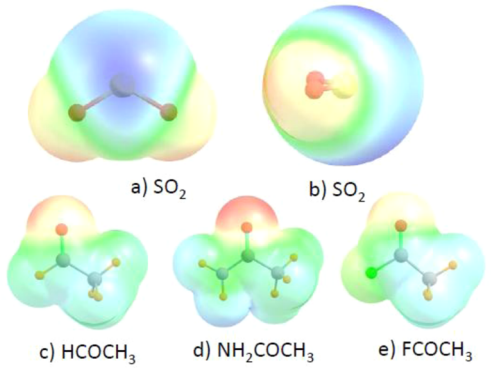

Figure 3. Electrostatic potentials of SO_2 (in (a) and perpendicular to (b) molecular plane) and three selected carbonyl partners at the MP2/aug-cc-pVDZ level. Red and blue regions indicate most negative and positive areas, respectively, varying between −0.05 and +0.05 au for SO_2, and −0.10 and +0.10 au for others. Contours illustrated on surface correspond to 1.5 times van der Waals radii.

surrounding SO_2 is generally positive (blue) around the S and negative (red) around the O atoms. As an important detail, the positive region is most intense above and below the molecular plane. The carbonyl-containing partners all have their negative region around the carbonyl O, and the remainder of the space is overall positive. These general features would lead to the expectation that the carbonyl O would be drawn toward the S of SO_2, especially to a region above the S atom, and this orientation is indeed the most commonly observed feature of the dimer geometries, facilitating the $O_{lp} \rightarrow \pi^*(SO)$ transfers of the S···O chalcogen bonds. As a secondary attraction, some of the positive regions around the carbonyl molecules would tend

dx.doi.org/10.1021/jp501932g | J. Phys. Chem. A 2014, 118, 3835−3845

Table 3. Maxima and Minima (kcal/mol) in Molecular Electrostatic Potential of Indicated Monomer, Lying on the Surface That Corresponds to Constant Electron Density of 0.001 au, at MP2/aug-cc-pVDZ Level

	maxima[a]			minima[b]	
SO_2	π(S) 31.25	—	—	O −17.88	S 19.01
1	π(C sp^2) 20.46	—	—	O (1) −32.94	O (2) −32.19
2	—	—	—	O −35.14	—
3	π(C sp^2) 16.32	σ(OH) 48.19	—	O (CO) −31.31	O (OH) −16.32
4	π(C sp^2) 13.37	σ(OCH_3) 14.81	—	O (CO) −33.38	O (OCH_3) −16.44
5	σ(NH1) 47.32	σ(NH2) 38.53	—	O −41.24	N −9.60
6	—	—	—	O −42.61	N −9.48
7	σ(COCH) 22.76	σ(CCH1) 20.37	σ(CCH2) 11.16	O −34.69	—
8	π(C sp^2) 25.42	σ(CH_3) 18.65	—	O −20.79	F −27.52
9	π(C sp^2) 23.10	σ(CH_3) 18.88	σ(CCl) 2.77	O −24.65	Cl −6.43
10	π(C sp^2) 23.50	σ(CH_3) 19.61	σ(CBr) 4.68	O −23.02	Cl −6.95
11	π(C sp^2) 15.36	σ(CH_3) 13.21	—	O (CO) −36.60	O (COC) −6.15
12	σ(NH) 54.10	—	—	O −54.57	—

[a]Maxima lie along indicated σ or π hole of atom. [b]Minima lie along lone pair directions.

toward the SO_2 O atoms, consistent with the CH···O HBs that occur in many cases.

The detailed structures of these MEPs are also helpful in understanding the relative energetics. Inspection of the red regions around the carbonyl O atoms in Figure 3 reveals that the replacement of the H in $HCOCH_3$ of Figure 3c by the NH_2 of Figure 3d results in a broader and more intense negative region. This observation is consistent with the greater strength of complex **5a** as compared to **1a**, as well as the notion that the amino group is electron-releasing. The reverse is true when F is substituted into the molecule, withdrawing electron density from the carbonyl in Figure 3e, and nearly eliminating the red region entirely. This less negative region weakens the interaction with SO_2, resulting in the weaker binding in **8a**.

These conclusions are not restricted to the three molecules in Figure 3. The magnification of the negative region around the carbonyl occurs not only for NH_2, but for all three of the N-containing molecules, as shown in Figure S1. Likewise, the electron withdrawal by F is repeated for the other halogens Cl and Br. And in the latter context, the potentials of these $XCOCH_3$ molecules do not show a substantial positive region along the extension of the C−X bond, whether X = F, Cl, or Br. This absence of a so-called σ-hole is consistent with the failure to observe any minima that contain a corresponding halogen bond.

The magnitudes of the potentials can be more quantitatively assessed by way of locating maxima and minima. The values of the potential at these points are reported in Table 3 on an isosurface that represents a total electron density of 0.001 au. The positive maxima are located either above the molecular plane (π-hole) or along the extension of a given σ-bond (σ-hole). The negative minima correspond to the lone pair directions of electronegative atoms. In the first place, the data in the third column of Table 3 confirm the very low positive potential along any purported halogen σ-hole for **8**, **9**, or **10**, if it exists at all. More importantly, the values of the MEP on the carbonyl O that participates in the chalcogen bond (column 4) confirm the qualitative picture described above and illustrated in Figure S1. Indeed, this value of the MEP is linearly related to the interaction energy, although the correlation coefficient is only 0.74.

It is worth stressing that this low correlation coefficient indicates that the MEP is not a perfect predictor of the binding strengths. This observation is not surprising when one realizes that the S···O bond is not the sole source of stability. Carboxyl substituent **3**, for example, is slightly more strongly bound by SO_2 than are **1** or **2**, but the potential around the carbonyl O of the former molecule is slightly less negative than those of the latter. The disproportionate strength of binding of **3** can be explained by a strong OH···O HB that supplements S···O.

Relationships between AIM and NBO Parameters. As indicated above, there are two principal kinds of noncovalent bonds present within these heterodimers. Within the total of 51 minima identified, the S···O chalcogen bond occurs 32 times (as defined by AIM) and DH···O HBs, (with D = C, O, or N) are observed 72 times. Based on past experience, one would expect the primary AIM determinants of these bonds (ρ and $\nabla^2\rho$ at the BCP) to correlate with the interatomic distance. And indeed, as illustrated in Figure 4a, there is an excellent linear correlation for S···O, with R^2 equal to 0.98 for ρ and 0.99 for its Laplacian; the correlations for the HBs are not quite as good: 0.96 and 0.90, respectively, graphically represented in Figure 4b. Note that ρ grows as the distance is shortened, while $-\nabla^2\rho$ becomes more negative. The ranges of ρ are comparable for the two sorts of bonds: 0.010−0.025 au for the chalcogen bonds, and 0.004−0.020 au for the HBs.[54]

The alternate determinant of the presence of a noncovalent bond derives from the NBO procedure. Figure 5a illustrates a rapid (nonlinear) growth in the NBO value of $E(2)$ as R(S···O) grows smaller. In fact, this relationship closely matches an exponential decay, with $E(2)$ proportional to distance. In addition to their relationships, there is some evidence in the literature that NBO parameter $E(2)$ can be correlated directly with AIM quantities ρ or $\nabla^2\rho$ in the case of intramolecular HBs, as for example in aldotetrose and aldopentonse sugars.[55−57] Figures 5b and 5c explore this relationship in the case of the chalcogen bonds. There is obviously a strong correlation between these various measures of bond strength, demonstrating that there is a relationship between methods of different nature: one topological (AIM) and another orbital (NBO).

DISCUSSION

The complexes between SO_2 and the various carbonyl-containing molecules are held together primarily by a S···O chalcogen bond, with smaller supplementary attractions from CH···O HBs. This chalcogen bond is fairly strong, with total binding energies varying between 4.2 and 8.6 kcal/mol. This

dx.doi.org/10.1021/jp501932g | J. Phys. Chem. A 2014, 118, 3835−3845

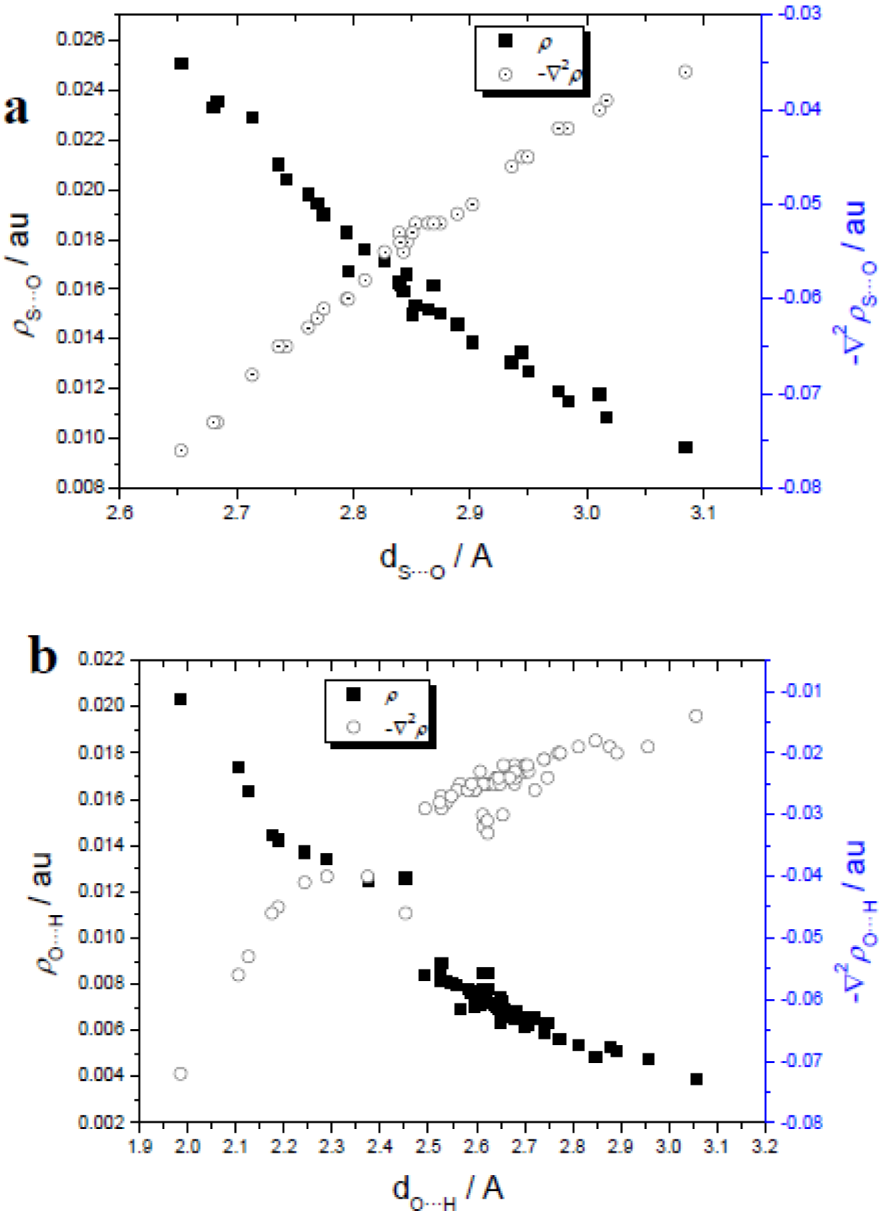

Figure 4. AIM topological variables at the BCP (ρ and $\nabla^2\rho$ in au) vs the interatomic distances (Å) between the atoms involved in (a) the chalcogen S···O and (b) HBs present in the heterodimers.

S···O bond occurs not only in the global minimum of each pair, but in the majority of secondary minima as well. There are occasional exceptions, such as the S···N or S···Br chalcogen bonds where the latter electronegative atoms replace O as electron donor. There are also cases where an OH···O or NH···O HBs appears when there is an OH or NH proton donor located on the carbonyl molecule. The S···O chalcogen bond is confirmed by a BCP between these two atoms in the AIM analysis of the wavefunction, whereas it is generally manifested in the NBO treatment via a carbonyl $O_{lp} \rightarrow \pi^*(SO)$ charge transfer. The AIM measures of bond strength, ρ and $\nabla^2\rho$, correlate fairly closely with the NBO value of $E(2)$, adding to the confidence in assessment of the strength of this bond, even in the presence of secondary attractive forces.

It should perhaps be stressed that the chalcogen bond at the heart of the bonding in these complexes differs in some important respects from another related sort of interaction, which is also usually referred to as a chalcogen bond. A common definition of a bond of this sort places a chalcogen atom such as S in a divalent bonding situation, as for example in HSF. An electron donor, D, is optimally positioned directly along the extension of one of the X−S bonds, which facilitates the transfer of charge from D into the X−S σ^* antibonding orbital, such that θ(X−S···D) tends toward 180°. The interaction is further stabilized by an electrostatic attraction between the negative potential surrounding donor D, and a positive region which also lies along an extension of the X−S bond.

The S···O chalcogen bond described in these complexes with SO_2 is different, first geometrically. The carbonyl O atom of the electron donor lies far from the S−O bond direction; in most cases, this O atom approaches the S atom from above, nearly perpendicular to the plane of SO_2. This absence of such an end-on attack can be traced to the electrostatic potential of SO_2 which Figure 3 shows to be negative along the extension of the S−O bond. Rather than donating charge to the σ^*(SO)

dx.doi.org/10.1021/jp501932g | J. Phys. Chem. A 2014, 118, 3835−3845

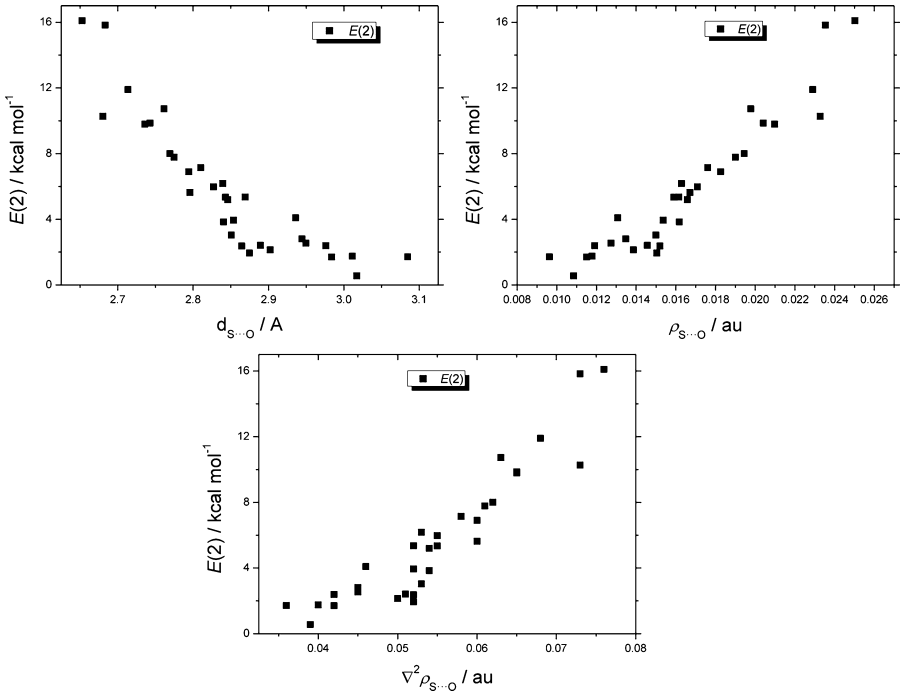

Figure 5. Second order NBO energy $E(2)$ (kcal/mol) vs the interatomic distances (Å) and the AIM topological variables at the BCP (ρ and $\nabla^2\rho$ in au) for the chalcogen S···O interactions present in the heterodimers.

antibond, it is the antibonding π^*(SO) bond which is the prime beneficiary. One simple way of distinguishing these two sorts of chalcogen bonds might be to refer to them as σ and π chalcogen bonds, respectively.

Inspection of the electrostatic potential surrounding each monomer aids in predicting and understanding the preferred intermolecular orientations and binding energies. The negative regions around the carbonyl O are drawn toward the positive area above and below the S atom of SO_2. Electron-releasing substituents such as NH_2 bolster the negative potential around the carbonyl O, thereby strengthening the S···O bond and the intermolecular attraction; vice versa for electron-withdrawing halogens. An auxiliary attraction arises between the negative O atoms of SO_2 and the positive regions about the partner molecule. The electrostatic potentials also explain the absence of halogen bonds in any of the dimer structures, since no positive region occurs along the extension of the C−X bond in $XCOCH_3$.

Substituents manifest their influence in a number of related ways. First, as mentioned above, an electron-withdrawing group will diminish the negatively charged area around the carbonyl O atom, thus reducing its electrostatic attraction with the positive region above and below the S atom of SO_2. A second consequence of withdrawing density toward a substituent will be a lowered availability of the carbonyl O lone pairs to donate charge to the SO_2 molecule. As a result, the N-containing molecules form the strongest interaction with SO_2, all greater than 8 kcal/mol; the weakest binding is associated with the halogenated carbonyls.

As shown here, altering the bonding character of the S atom from a pair of single bonds, as in HSH or FSH, to multiple bonds in SO_2 changes the geometry and character of the chalcogen bond. Rather than approaching the S atom along the FS bond direction, an electron donor prefers a perpendicular approach to SO_2, above the molecular plane. One may consider certain analogies to the halogen bond. A monovalent halogen atom X draws an electron donor to an extension of the C−X bond. Unlike S, however, this same geometry is preferred also for hypervalent halogen atoms such as BrF_3[58] or $FBrO_3$,[59] with the charge being transferred into a σ^* orbital regardless of the bonding pattern around the halogen.

Pnicogens like P can also engage in multiple bonds. Calculations of $XP{=}CH_2$ dimers[60] indicate the approach of one molecule toward the other along the projection of a bond axis, i.e., traditional pnicogen bonds. There were several alternate minima observed with stacked parallel geometries, but their bonding was attributed to π-stacking, rather than any sort of pnicogen bond. Other complexes involving $XP{=}CH_2$[61] manifested orientations that place the partner molecule along the extension of one of the P bonds in most cases, and others where the partner approaches the P from above the $XP{=}CH_2$ molecular plane. However, the $XP{=}CH_2$ acts primarily as electron donor in these perpendicular complexes, rather than as the acceptors in the SO_2 complexes examined here. XPO_2 molecules also attract a base toward the region above the P atom, but the charge is transferred to the σ^* orbitals of XPO_2, rather than to π^*.[62]

Returning finally to the original questions posed in the introduction, the S··O chalcogen bond remains the dominant attractive interaction even as the H atoms of H_2CO are replaced by various substituents. The strength of the bond is influenced primarily by the inductive effect of the substituent. Electron-withdrawing halogens reduce the binding energy while the interaction is strengthened by the amide functionality. The largest interaction energy encountered here is 8.6 kcal/mol, and occurs when SO_2 is paired with the $(CH_3)_2NCOCH_3$ amide. This value places the chalcogen bond squarely in the range of some of the strongest H and halogen bonds.

dx.doi.org/10.1021/jp501932g | J. Phys. Chem. A 2014, 118, 3835−3845

■ ASSOCIATED CONTENT

Supporting Information

MEP of all monomers and geometries of all minima, both global and secondary, as well as their detailed NBO analysis. This material is available free of charge via the Internet at http://pubs.acs.org.

■ AUTHOR INFORMATION

Corresponding Author

*Fax: (+1) 435-797-3390. E-mail: steve.scheiner@usu.edu.

Notes

The authors declare no competing financial interest.

■ ACKNOWLEDGMENTS

This work has been supported by NSF-CHE-1026826. L.M.A. thanks the MICINN for a PhD grant (No. BES−2010−031225) and the MINECO (Project No. CTQ2012−35513−C02−02) for continuing support. Computer, storage, and other resources from the Division of Research Computing in the Office of Research and Graduate Studies at Utah State University and the CTI (CSIC) are gratefully acknowledged. Gratitude is also due to Prof. Ibon Alkorta from IQM (CSIC) for the NBO analysis with the NBO6.0 program.

■ REFERENCES

(1) Auffinger, P.; Hays, F. A.; Westhof, E.; Ho, P. S. Halogen Bonds in Biological Molecules. *Proc. Natl. Acad. Sci. U.S.A.* **2004**, *101*, 16789−16794.

(2) Legon, A. C. The Halogen Bond: An Interim Perspective. *Phys. Chem. Chem. Phys.* **2010**, *12*, 7736−7747.

(3) Erdelyi, M. Halogen Bonding in Solution. *Chem. Soc. Rev.* **2012**, *41*, 3547−3557.

(4) Scheiner, S. Sensitivity of Noncovalent Bonds to Intermolecular Separation: Hydrogen, Halogen, Chalcogen, and Pnicogen Bonds. *CrystEngComm* **2013**, *15*, 3119−3124.

(5) Hauchecorne, D.; Herrebout, W. A. Experimental Characterization of C−X···Y−C (X = Br, I; Y = F, Cl) Halogen−Halogen Bonds. *J. Phys. Chem. A* **2013**, *117*, 11548−11557.

(6) Riley, K.; Murray, J.; Fanfrlík, J.; Řezáč, J.; Solá, R.; Concha, M.; Ramos, F.; Politzer, P. Halogen Bond Tunability II: The Varying Roles of Electrostatic and Dispersion Contributions to Attraction in Halogen Bonds. *J. Mol. Model.* **2013**, *19*, 4651−4659.

(7) Vener, M. V.; Shishkina, A. V.; Rykounov, A. A.; Tsirelson, V. G. Cl···Cl Interactions in Molecular Crystals: Insights from the Theoretical Charge Density Analysis. *J. Phys. Chem. A* **2013**, *117*, 8459−8467.

(8) Solimannejad, M.; Malekani, M.; Alkorta, I. Substituent Effects on the Cooperativity of Halogen Bonding. *J. Phys. Chem. A* **2013**, *117*, 5551−5557.

(9) Stone, A. J. Are Halogen Bonded Structures Electrostatically Driven? *J. Am. Chem. Soc.* **2013**, *135*, 7005−7009.

(10) Evangelisti, L.; Feng, G.; Gou, Q.; Grabow, J.-U.; Caminati, W. Halogen Bond and Free Internal Rotation: The Microwave Spectrum of CF_3Cl−Dimethyl Ether. *J. Phys. Chem. A* **2014**, *118*, 579−582.

(11) Moilanen, J.; Ganesamoorthy, C.; Balakrishna, M. S.; Tuononen, H. M. Weak Interactions between Trivalent Pnictogen Centers: Computational Analysis of Bonding in Dimers $X_3E\cdots EX_3$ (E = Pnictogen, X = Halogen). *Inorg. Chem.* **2009**, *48*, 6740−6747.

(12) Zahn, S.; Frank, R.; Hey-Hawkins, E.; Kirchner, B. Pnicogen Bonds: A New Molecular Linker? *Chem.—Eur. J.* **2011**, *17*, 6034−6038.

(13) Bühl, M.; Kilian, P.; Woollins, J. D. Prediction of a New Delocalised Bonding Motif between Group 15 or Group 16 Atoms. *ChemPhysChem* **2011**, *12*, 2405−2408.

(14) Scheiner, S. A New Noncovalent Force: Comparison of P···N Interaction with Hydrogen and Halogen Bonds. *J. Chem. Phys.* **2011**, *134*, 094315.

(15) Scheiner, S. Effects of Substituents upon the P···N Noncovalent Interaction: The Limits of Its Strength. *J. Phys. Chem. A* **2011**, *115*, 11202−11209.

(16) Adhikari, U.; Scheiner, S. Effects of Carbon Chain Substituents on the P···N Noncovalent Bond. *Chem. Phys. Lett.* **2012**, *536*, 30−33.

(17) Alkorta, I.; Elguero, J.; Del Bene, J. E. Pnicogen-Bonded Cyclic Trimers $(PH_2X)_3$ with X = F, Cl, OH, NC, CN, CH_3, H, and BH_2. *J. Phys. Chem. A* **2013**, *117*, 4981−4987.

(18) Sánchez-Sanz, G.; Alkorta, I.; Trujillo, C.; Elguero, J. Intramolecular Pnicogen Interactions in PHF−$(CH_2)_n$−PHF (n=2−6) Systems. *ChemPhysChem* **2013**, *14*, 1656−1665.

(19) Liu, X.; Cheng, J.; Li, Q.; Li, W. Competition of Hydrogen, Halogen, and Pnicogen Bonds in the Complexes of HArF with XH_2P (X═F, Cl, and Br). *Spectrochim. Acta, Part A* **2013**, *101*, 172−177.

(20) Scheiner, S. The Pnicogen Bond: Its Relation to Hydrogen, Halogen, and Other Noncovalent Bonds. *Acc. Chem. Res.* **2012**, *46*, 280−288.

(21) Nagao, Y.; Hirata, T.; Goto, S.; Sano, S.; Kakehi, A.; Iizuka, K.; Shiro, M. Intramolecular Nonbonded S···O Interaction Recognized in (Acylimino)thiadiazoline Derivatives as Angiotensin II Receptor Antagonists and Related Compounds. *J. Am. Chem. Soc.* **1998**, *120*, 3104−3110.

(22) Iwaoka, M.; Takemoto, S.; Tomoda, S. Statistical and Theoretical Investigations on the Directionality of Nonbonded S···O Interactions. Implications for Molecular Design and Protein Engineering. *J. Am. Chem. Soc.* **2002**, *124*, 10613−10620.

(23) Werz, D. B.; Gleiter, R.; Rominger, F. Nanotube Formation Favored by Chalcogen−Chalcogen Interactions. *J. Am. Chem. Soc.* **2002**, *124*, 10638−10639.

(24) Sanz, P.; Mo, O.; Yanez, M. Characterization of Intramolecular Hydrogen Bonds and Competitive Chalcogen-Chalcogen Interactions on the Basis of the Topology of the Charge Density. *Phys. Chem. Chem. Phys.* **2003**, *5*, 2942−2947.

(25) Bleiholder, C.; Werz, D. B.; Köppel, H.; Gleiter, R. Theoretical Investigations on Chalcogen−Chalcogen Interactions: What Makes These Nonbonded Interactions Bonding? *J. Am. Chem. Soc.* **2006**, *128*, 2666−2674.

(26) Junming, L.; Yunxiang, L.; Subin, Y.; Weiliang, Z. Theoretical and Crystallographic Data Investigations of Noncovalent S···O Interactions. *Struct. Chem.* **2011**, *22*, 757−763.

(27) Adhikari, U.; Scheiner, S. Sensitivity of Pnicogen, Chalcogen, Halogen and H-Bonds to Angular Distortions. *Chem. Phys. Lett.* **2012**, *532*, 31−35.

(28) Sánchez-Sanz, G.; Trujillo, C.; Alkorta, I.; Elguero, J. Intermolecular Weak Interactions in HTeXH Dimers (X═O, S, Se, Te): Hydrogen Bonds, Chalcogen−Chalcogen Contacts and Chiral Discrimination. *ChemPhysChem* **2012**, *13*, 496−503.

(29) Iwaoka, M.; Isozumi, N. Hypervalent Nonbonded Interactions of a Divalent Sulfur Atom. Implications in Protein Architecture and the Functions. *Molecules* **2012**, *17*, 7266−7283.

(30) Wang, X.-Y.; Jiang, W.; Chen, T.; Yan, H.-J.; Wang, Z.-H.; Wan, L.-J.; Wang, D. Molecular Evidence for the Intermolecular SS Interaction in the Surface Molecular Packing Motifs of a Fused Thiophene Derivative. *Chem. Commun.* **2013**, *49*, 1829−1831.

(31) Bauza, A.; Quinonero, D.; Deya, P. M.; Frontera, A. Halogen Bonding versus Chalcogen and Pnicogen Bonding: A Combined Cambridge Structural Database and Theoretical Study. *CrystEngComm* **2013**, *15*, 3137−3144.

(32) Bauzá, A.; Mooibroek, T. J.; Frontera, A. Tetrel-Bonding Interaction: Rediscovered Supramolecular Force? *Angew. Chem., Int. Ed.* **2013**, *52*, 12317−12321.

(33) Mani, D.; Arunan, E. The X-CY (X = O/F, Y = O/S/F/Cl/Br/N/P) 'Carbon Bond' and Hydrophobic Interactions. *Phys. Chem. Chem. Phys.* **2013**, *15*, 14377−14383.

(34) Donald, K. J.; Tawfik, M. The Weak Helps the Strong: Sigma-Holes and the Stability of MF_4·Base Complexes. *J. Phys. Chem. A* **2013**, *117*, 14176−14183.
(35) Grabowski, S. J. Tetrel Bond-σ-Hole Bond as a Preliminary Stage of the S_N2 Reaction. *Phys. Chem. Chem. Phys.* **2014**, *16*, 1824−1834.
(36) Azofra, L. M.; Scheiner, S. Complexes Containing CO_2 and SO_2. Mixed Dimers, Trimers and Tetramers. *Phys. Chem. Chem. Phys.* **2014**, *16*, 5142−5149.
(37) Azofra, L. M.; Scheiner, S. Complexation of n SO_2 Molecules (n = 1, 2, 3) with Formaldehyde and Thioformaldehyde. *J. Chem. Phys.* **2014**, *140*, 034302.
(38) Murray, J.; Lane, P.; Clark, T.; Riley, K.; Politzer, P. σ-Holes, π-Holes and Electrostatically-driven Interactions. *J. Mol. Model.* **2012**, *18*, 541−548.
(39) Altarsha, M.; Ingrosso, F.; Ruiz-Lopez, M. F. A New Glimpse into the CO_2-Philicity of Carbonyl Compounds. *ChemPhysChem* **2012**, *13*, 3397−3403.
(40) Azofra, L. M.; Altarsha, M.; Ruiz-López, M. l. F.; Ingrosso, F. A Theoretical Investigation of the CO_2-Philicity of Amides and Carbamides. *Theor. Chem. Acc.* **2013**, *132*, 1326.
(41) Møller, C.; Plesset, M. S. Note on an Approximation Treatment for Many-Electron Systems. *Phys. Rev.* **1934**, *46*, 618−622.
(42) Dunning, T. H. Gaussian Basis Sets for the Atoms Gallium through Krypton. *J. Chem. Phys.* **1977**, *66*, 1382−1383.
(43) Dunning, T. H. J. Gaussian Basis Sets for Use in Correlated Molecular Calculations. I. The Atoms Boron Through Neon and Hydrogen. *J. Chem. Phys.* **1989**, *90*, 1007−1023.
(44) Woon, D. E.; Dunning, T. H. Gaussian Basis Sets for Use in Correlated Molecular Calculations. III. The Atoms Aluminum through Argon. *J. Chem. Phys.* **1993**, *98*, 1358−1371.
(45) Sergeeva, A. P.; Averkiev, B. B.; Zhai, H.-J.; Boldyrev, A. I.; Wang, L.-S. All-boron Analogues of Aromatic Hydrocarbons: B_{17}^- and B_{18}^-. *J. Chem. Phys.* **2011**, *134*, 224304.
(46) Frisch, M. J.; Trucks, G. W.; Schlegel, H. B.; Scuseria, G. E.; Robb, M. A.; Cheeseman, J. R.; Scalmani, G.; Barone, V.; Mennucci, B.; Petersson, G. A.; Nakatsuji, H.; Caricato, M.; Li, X.; Hratchian, H. P.; Izmaylov, A. F.; Bloino, J.; Zheng, G.; Sonnenberg, J. L.; Hada, M.; Ehara, M.; Toyota, K.; Fukuda, R.; Hasegawa, J.; Ishida, M.; Nakajima, T.; Honda, Y.; Kitao, O.; Nakai, H.; Vreven, T.; Montgomery, J.; J, A.; Peralta, J. E.; Ogliaro, F.; Bearpark, M.; Heyd, J. J.; Brothers, E.; Kudin, K. N.; Staroverov, V. N.; Kobayashi, R.; Normand, J.; Raghavachari, K.; Rendell, A.; Burant, J. C.; Iyengar, S. S.; Tomasi, J.; Cossi, M.; Rega, N.; Millam, N. J.; Klene, M.; Knox, J. E.; Cross, J. B.; Bakken, V.; Adamo, C.; Jaramillo, J.; Gomperts, R.; Stratmann, R. E.; Yazyev, O.; Austin, A. J.; Cammi, R.; Pomelli, C.; Ochterski, J. W.; Martin, R. L.; Morokuma, K.; Zakrzewski, V. G.; Voth, G. A.; Salvador, P.; Dannenberg, J. J.; Dapprich, S.; Daniels, A. D.; Farkas, Ö.; Foresman, J. B.; Ortiz, J. V.; Cioslowski, J.; Fox, D. J. *Guassian09*; Gaussian, Inc., Wallingford, CT, 2009.
(47) Bader, R. F. W. *Atoms in Molecules: A Quantum Theory*; Clarendon Press: Oxford, UK, 1990.
(48) Popelier, P. L. A. *Atoms In Molecules, An Introduction*; Prentice Hall: Harlow, UK, 2000.
(49) Weinhold, F.; Landis, C. R. *Valency and Bonding. A Natural Bond Orbital Donor-Aceptor Perspective*; Cambridge Press: Cambridge, UK, 2005.
(50) Chai, J.-D.; Head-Gordon, M. Long-range Corrected Hybrid Density Functionals with Damped Atom-Atom Dispersion Corrections. *Phys. Chem. Chem. Phys.* **2008**, *10*, 6615−6620.
(51) Keith, T. A. *AIMA11*; TK Gristmill Software, Overland Park, KS, USA, 2013.
(52) Glendening, E. D.; Badenhoop, J. K.; Reed, A. E.; Carpenter, J. E.; Bohmann, J. A.; Morales, C. M.; Landis, C. R.; Weinhold, F. *NBO6.0*; Theoretical Chemistry Institute, University of Wisconsin, Madison, WI, USA, 2013.
(53) Politzer, P.; Murray, J.; Concha, M. σ-Hole Bonding between Like Atoms; A Fallacy of Atomic Charges. *J. Mol. Model.* **2008**, *14*, 659−665.
(54) Koch, U.; Popelier, P. L. A. Characterization of C-H-O Hydrogen-Bonds on the Basis of the Charge-Density. *J. Phys. Chem.* **1995**, *99*, 9747−9754.
(55) Azofra, L. M.; Alkorta, I.; Elguero, J.; Popelier, P. L. A. Conformational Study of the Open-Chain and Furanose Structures of D-Erythrose and D-Threose. *Carbohydr. Res.* **2012**, *358*, 96−105.
(56) Quesada-Moreno, M. M.; Azofra, L. M.; Avilés-Moreno, J. R.; Alkorta, I.; Elguero, J.; López-González, J. J. Conformational Preference and Chiroptical Response of Carbohydrates D-Ribose and 2-Deoxy-D-ribose in Aqueous and Solid Phases. *J. Phys. Chem. B* **2013**, *117*, 14599−14614.
(57) Azofra, L. M.; Quesada-Moreno, M. M.; Alkorta, I.; Avilés-Moreno, J. R.; López-González, J. J.; Elguero, J. Carbohydrates in the Gas Phase: Conformational Preference of D-Ribose and 2-Deoxy-D-ribose. *New J. Chem.* **2014**, *38*, 529−538.
(58) Wang, W. Halogen Bond Involving Hypervalent Halogen: CSD Search and Theoretical Study. *J. Phys. Chem. A* **2011**, *115*, 9294−9299.
(59) Cheng, N.; Bi, F.; Liu, Y.; Zhang, C.; Liu, C. The Structures and Properties of Halogen Bonds Involving Polyvalent Halogen in Complexes of FXO_n (X = Cl, Br; n = 0−3)-CH_3CN. *New J. Chem.* **2014**, *38*, 1256−1263.
(60) Del Bene, J. E.; Alkorta, I.; Elguero, J. Characterizing Complexes with Pnicogen Bonds Involving sp^2 Hybridized Phosphorus Atoms: $(H_2C{=}PX)_2$ with X = F, Cl, OH, CN, NC, CCH, H, CH_3, and BH_2. *J. Phys. Chem. A* **2013**, *117*, 6893−6903.
(61) Del Bene, J. E.; Alkorta, I.; Elguero, J. Properties of Complexes $H_2C{=}(X)P{:}PXH_2$, for X = F, Cl, OH, CN, NC, CCH, H, CH_3, and BH_2: P···P Pnicogen Bonding at σ-Holes and π-Holes. *J. Phys. Chem. A* **2013**, *117*, 11592−11604.
(62) Alkorta, I.; Elguero, J.; Del Bene, J. E. Pnicogen Bonded Complexes of PO_2X (X = F, Cl) with Nitrogen Bases. *J. Phys. Chem. A* **2013**, *117*, 10497−10503.